Cellular/Molecular

Mrgprd-Expressing Polymodal Nociceptive Neurons Innervate Most Known Classes of Substantia Gelatinosa Neurons

Hong Wang and Mark J. Zylka

Department of Cell and Molecular Physiology, University of North Carolina Neuroscience Center, University of North Carolina, Chapel Hill, North Carolina 27599

The *Mas-related G-protein-coupled receptor D* (*Mrgprd*) marks a distinct subset of sensory neurons that transmit polymodal nociceptive information from the skin epidermis to the substantia gelatinosa (SG, lamina II) of the spinal cord. Moreover, *Mrgprd*-expressing (*Mrgprd*$^+$) neurons are required for the full expression of mechanical but not thermal nociception. While such anatomical and functional specificity suggests *Mrgprd*$^+$ neurons might synapse with specific postsynaptic targets in the SG, precisely how *Mrgprd*$^+$ neurons interface with spinal circuits is currently unknown. To study circuit connectivity, we genetically targeted the light-activated ion channel Channelrhodopsin-2-Venus (ChR2-Venus) to the *Mrgprd* locus. In these knock-in mice, ChR2-Venus was localized to nonpeptidergic *Mrgprd*$^+$ neurons and axons, while peptidergic CGRP$^+$ neurons were not significantly labeled. Dissociated *Mrgprd*$^+$ DRG neurons from mice expressing one or two copies of ChR2-Venus could be activated *in vitro* as evidenced by light-evoked currents and action potentials. In addition, illumination of *Mrgprd-ChR2-Venus*$^+$ axon terminals in spinal cord slices evoked EPSCs in half of all SG neurons. Within this subset, *Mrgprd*$^+$ neurons were monosynaptically connected to most known classes of SG neurons, including radial, tonic central, transient central, vertical, and antenna cells. This cellular diversity ruled out the possibility that *Mrgprd*$^+$ neurons innervate a dedicated class of SG neuron. Our findings set broad constraints on the types of spinal neurons that process afferent input from *Mrgprd*$^+$ polymodal nociceptors.

Introduction

In mammals, pain-producing stimuli are detected by nociceptive neurons whose cell bodies are located in the dorsal root ganglia (DRGs) and trigeminal ganglia. Most nociceptive neurons can be divided into peptidergic and nonpeptidergic subsets, with peptidergic neurons marked by the neuropeptide calcitonin gene-related peptide (CGRP) and nonpeptidergic neurons marked by the isolectin B4 (IB4) (Molliver et al., 1997; Hunt and Mantyh, 2001; Woolf and Ma, 2007). Nociceptive neurons are activated peripherally by noxious thermal, mechanical, and chemical stimuli (Perl, 1996). Following activation, nociceptive signals are relayed from the dorsal horn of the spinal cord to the brain, where pain is perceived.

The G-protein-coupled receptor (GPCR) *Mrgprd* molecularly marks ~75% of all IB4$^+$ nonpeptidergic nociceptive neurons and these *Mrgprd*$^+$ neurons exclusively innervate skin and terminate in lamina II (the substantia gelatinosa or SG) of dorsal spinal cord (Dong et al., 2001; Zylka et al., 2003, 2005). Within the skin, *Mrgprd*$^+$ neurons innervate the most superficial layer of epidermis, the stratum granulosum, while peptidergic CGRP$^+$ neurons innervate the underlying stratum spinosum. These anatomical differences suggest *Mrgprd*$^+$ neurons might have unique sensory functions. Indeed, dissociated *Mrgprd*$^+$ neurons respond selectively to extracellular ATP in culture and have physiological properties that are typical of nociceptors (Dussor et al., 2008). Moreover, ablation of *Mrgprd*$^+$ neurons produces selective deficits in behavioral responses to mechanical stimuli (Cavanaugh et al., 2009) even though *Mrgprd*$^+$ neurons respond to noxious thermal and mechanical stimuli (Rau et al., 2009). Conversely, the capsaicin and noxious heat receptor TRPV1 is found in many peptidergic CGRP$^+$ neurons and ablation of TRPV1$^+$ spinal terminals produces selective deficits in behavioral responses to noxious thermal stimuli (Karai et al., 2004; Cavanaugh et al., 2009). While these studies suggest that behaviorally relevant stimulus modalities are first segregated at the primary afferent level, these studies also raise the question of how modality-selective information remains segregated at higher levels in the nervous system.

Received July 8, 2009; revised Sept. 9, 2009; accepted Sept. 10, 2009.

This work was supported by University of North Carolina (UNC) startup funds, grants to M.J.Z. from The Sloan Foundation, The Searle Scholars Program, The Klingenstein Foundation, The Whitehall Foundation, the Rita Allen Foundation, and the National Institute of Neurological Disorders and Stroke (NINDS) (R01NS060725). Confocal imaging was performed at the UNC-Chapel Hill Confocal Imaging Facility, which is cofunded by NINDS and the Eunice Kennedy Shriver National Institute of Child Health and Human Development (P30NS045892). M.J.Z. is a Rita Allen Foundation Milton E. Cassel Scholar. We thank Ben Philpot and Edward Perl for comments on this manuscript, Edward Perl and Jihong Zheng for teaching us how to perform spinal cord slice electrophysiology, Karl Deisseroth for providing codon-optimized ChR2, Randy Thresher and Stephen Knight at the UNC Animal Models Core Facility for embryonic stem cell work and blastocyst injections, Bonnie Taylor-Blake for all histology and confocal imaging, and Yvette Chuang for technical assistance.

Correspondence should be addressed to Mark J. Zylka, Department of Cell and Molecular Physiology, University of North Carolina Neuroscience Center, University of North Carolina, CB #7545, 115 Mason Farm Road, Chapel Hill, NC 27599. E-mail: zylka@med.unc.edu.

DOI:10.1523/JNEUROSCI.3248-09.2009

 0270-6474/09/2913202-08$15.00/0

To study *Mrgprd*$^+$ neuron connectivity at the spinal level, we genetically targeted ChR2-Venus to the *Mrgprd* locus by homologous recombination. ChR2 is a blue light-gated ion channel that can be used to activate neurons with millisecond precision (Nagel et al., 2003; Boyden et al., 2005; Li et al., 2005; Bi et al., 2006; Arenkiel et al., 2007; Hwang et al., 2007; Campagnola et al., 2008). In addition, photostimulation of ChR2 can be used to map circuit connectivity (Petreanu et al., 2007; Wang et al., 2007; Zhang and Oertner, 2007; Liewald et al., 2008). Our studies with ChR2 reveal that *Mrgprd*$^+$ neurons innervate ~50% all SG neurons, including monosynaptic connections with most known cell types in the SG. This finding suggests *Mrgprd*$^+$ sensory input is processed by afferent-selective modules made up of diverse SG cell types. This modular organization has implications for how modality-selective sensory information is segregated within the dorsal spinal cord. Moreover, our findings extend previous studies showing that circuitry within the SG is modular and highly organized (Lu and Perl, 2003, 2005; Yasaka et al., 2007; Kato et al., 2009).

Materials and Methods

All procedures involving vertebrate animals were approved by the Institutional Animal Care and Use Committee at the University of North Carolina at Chapel Hill.

Generation of Mrgprd-ChR2-Venus *knock-in mice.* The arms of the *Mrgprd* targeting construct were subcloned from a 129/SvJ genomic DNA BAC and amino acids # 2–315 were eliminated from the 321 amino acid coding region of *Mrgprd* (GenBank accession # AAK91800). Mammalian codon-optimized ChR2(H134R)Venus, described by Campagnola et al. (2008), followed by a self-excising loxP-flanked pol-II promoter-neomycin resistance cassette (ACN) (Bunting et al., 1999) was ligated in-frame to the start codon of *Mrgprd*. Homologous recombination was performed in mouse E14 embryonic stem cells following standard procedures. Correctly targeted cells were identified by Southern blot hybridization using probes that flanked the 5′ and 3′ arms of the targeting constructs, as well as an internal neomycin probe. Chimeric mice were produced by blastocyst injection and mated to C57BL/6 mice to establish the line. Tissue was obtained from mice that were backcrossed to C57BL/6 mice for two generations. As previously reported, deletion of *Mrgprd* did not affect viability or result in obvious anatomical or behavioral abnormalities (Zylka et al., 2005).

Mrgprd-ChR2-Venus mice were genotyped by PCR amplification of tail genomic DNA with primers (MrgD-2: 5′ GGATCATGACCGGCATGAAGATC; MrgD-9: 5′ GGTAGATTCAGGCACAGTGGGAG; hChR2_Arg2: 5′ GTGAGGTTGCTCAGGCGGATAAGGATGACAG). These primers detected the wild-type allele (668 bp) and knock-in allele (500 bp).

Cell culture. DRG neurons from all spinal levels were dissected from postnatal day 30–60 mice and cultured with 100 nM all-trans retinal as described previously (Campagnola et al., 2008).

Histology. Adult male mice, 6–12 weeks of age, were killed by cervical dislocation, decapitation or pentobarbital overdose. Lumbar spinal cord, DRGs (L4–L6) and skin were dissected then immersion-fixed for 8, 4, and 3 h, respectively, in 4% paraformaldehyde, 0.1 M phosphate buffer, pH 7.4. Tissues were cryoprotected in 30% sucrose, 0.1 M phosphate buffer, pH 7.3 at 4°C for 24–48 h, frozen in OCT, sectioned with a cryostat at 20 μm, and mounted on Superfrost Plus slides. Slides were stored at −20°C. Alternatively, free-floating sections were sectioned at 30 μm and immediately stained.

Immunofluorescence was performed using antibodies and procedures as previously described (Zylka et al., 2005, 2008). We used high-salt TBS+TX (50 mM Tris, 2.7% NaCl, 0.3% Triton X-100, pH 7.6) in all wash and antibody incubation steps. To stain nuclei, 1:10,000 Draq5 was added to the secondary antibody mixture. The avidin–biotin complex reaction with Texas red was used to visualize cells labeled with biocytin during whole-cell recordings. Images were obtained using a Zeiss LSM 510 NLO confocal microscope.

Photostimulation. We used an Intensilight mercury fiber illuminator (Nikon), an Improvision Microshutter and Shutter hub under TTL pulse control and the Semrock BriteLine FITC-3540B filter set (exciter: 482 ± 18 nm; emitter: 563 ± 20 nm; dichroic: 446–500 nm reflection band, 513–725 nm transmission band).

Electrophysiology. ChR2-Venus-expressing DRG neurons were identified using an epifluorescence microscope (Nikon Eclipse FN1) equipped with a 40× water-immersion objective (NIR Apo 40×/0.80W, Nikon). Neurons were perfused during recording in oxygenated (95% O_2, 5% CO_2) bath solution at room temperature consisting of the following (in mM): 10 HEPES, 140 NaCl, 4 KCl, 2 $MgCl_2$, 2 $CaCl_2$, 5 glucose, pH 7.4, 300 mOsM. Pipette solution for DRG neurons and SG neurons contained the following (in mM): 130 potassium gluconate, 5 NaCl, 1 $CaCl_2$, 1 $MgCl_2$, 11 EGTA, 10 HEPES, 4 NaATP; pH was adjusted to 7.3 with KOH, and osmolarity was 295 mOsM. Patch pipettes for DRG and SG neurons were made of borosilicate glass and had a resistance of 3–6 MΩ when filled with pipette solution.

Patch-clamp recordings of spinal cord slices were performed as described previously (Grudt and Perl, 2002; Hantman et al., 2004), with minor modifications. Briefly, mice (28–56 d old) were deeply anesthetized with urethane (1.5 g/kg, i.p.). The lumbar spinal cord was quickly dissected and slices (450–500 μm thick) were prepared using a Vibratome 3000 EP in cutting solution containing the following (in mM): 75 sucrose, 80 NaCl, 2.5 KCl, 0.5 $CaCl_2$, 7 $MgCl_2$, 1.25 NaH_2PO_4, 25 $NaHCO_3$). Slices were incubated at 37°C for 45 min in artificial CSF (ACSF) containing the following (in mM): 125 NaCl, 2.5 KCl, 2.0 $CaCl_2$, 1.0 $MgCl_2$, 1.25 NaH_2PO_4, 26 $NaHCO_3$, 25 D-glucose, pH 7.4. Slices were then incubated at room temperature until recording. All solutions were bubbled with 95% O_2 and 5% CO_2 during the cutting and incubation steps described above.

Spinal cord slices were superfused with ACSF bubbled with 95% O_2 and 5% CO_2 at room temperature (6–10 ml/min) in a recording chamber mounted on a Nikon FN1 microscope. Infrared–differential interference contrast (IR-DIC) illumination was used to visualize neurons in the SG for patch-clamp recordings. *Mrgprd*$^+$ afferents terminate in the SG (Fig. 1*E*, lamina II) (Zylka et al., 2005).

Physiological and morphological characterization of SG neurons. We physiologically and morphologically characterized SG neurons using previously described procedures and cell type designations (Grudt and Perl, 2002; Lu and Perl, 2003, 2005; Maxwell et al., 2007; Yasaka et al., 2007). Briefly, sagittal slices (450–500 μm thick) with one dorsal root attached were cut from mouse spinal cord (28–56 d old) and whole-cell recordings were made from SG neurons as described above except pipettes were backfilled with pipette solution containing 0.5% biocytin. The firing pattern of each neuron was determined to 1 s depolarizing pulses (−60 to −20 mV) from a holding potential of −60 mV in current-clamp mode. We then switched to voltage-clamp mode and photostimulated the recorded cell with five 1000 ms pulses of blue light (1 min interpulse interval). We monitored series resistance during recording and discarded cells if resistance changed by >20%. Dorsal root conduction velocity was estimated from the latency of the EPSCs and the conduction distance. Following immersion fixation of slices, we visualized biocytin-filled neurons with streptavidin–Texas red and confocal microscopy.

SG neuron types were defined as follows. (1) Radial cell: For radial cells, dendrites extend in all directions relative to soma and lack distinctive electrophysiological characteristics. (2) Tonic central cell: Tonic central cells fire action potentials regularly during the full duration of a depolarizing current. On confocal reconstruction, dendritic tree extends ~300 μm rostral–caudally from the cell soma and <60 μm in the dorsal–ventral plane. (3) Transient central cell: Transient central cells promptly but transiently fire one or a few action potentials following step depolarization. Dendritic tree is oriented rostral–caudally and extends ~300 μm in a sagittal plane from the cell soma. (4) Vertical cell: Most vertical cells show delayed discharge of action potentials to step depolarization and spike frequency adaptation. Dendritic distribution is primarily ventral to the cell soma. (5) Islet cell: Islet cells tonically fire action potentials during maintained depolarization, exhibit a short latency to the first spike, and show little to no spike frequency adaptation. Dendritic

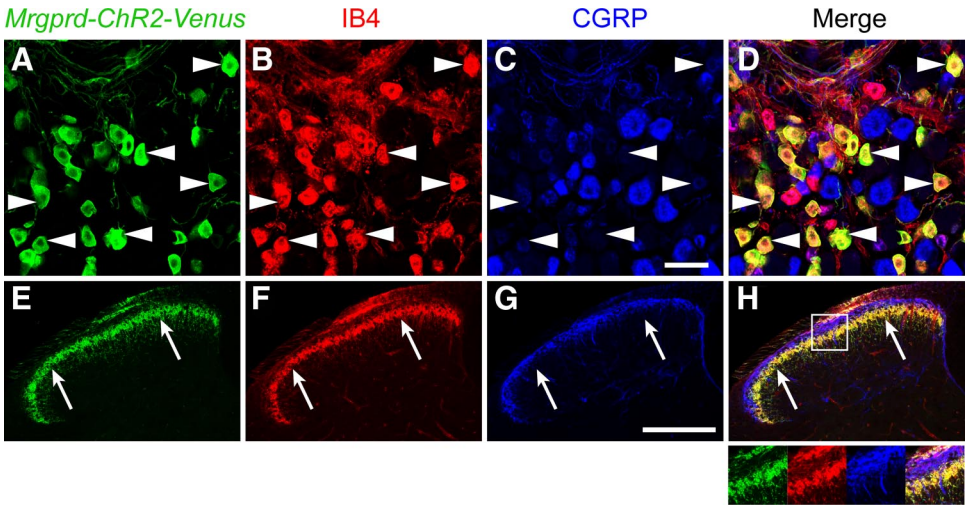

Figure 1. Localization of *Mrgprd-ChR2-Venus* to nonpeptidergic neurons and their axon terminals. ***A–H***, L4 –L6 DRG neurons (***A–D***) and lumbar spinal cord (***E–H***) from *Mrgprd-ChR2-Venus*$^{+/-}$ mice were stained with antibodies against GFP (green; anti-GFP antibodies detect Venus because Venus is virtually identical to GFP at the amino acid level), the lectin IB4 (red) and with antibodies against CGRP (blue). Examples of *Mrgprd-ChR2-Venus* neurons that bind IB4 are indicated (arrowheads). Arrows mark the ventral boundary of lamina II. Inset in ***H*** is magnified at the bottom right. Images were acquired by confocal microscopy. Scale bars: ***A–D***, 50 μm; ***E–H***, 200 μm.

trees extend in the rostral–caudal direction at least 400 μm on each side of the cell body with particularly extensive dendritic branching. (6) Antenna cell: The cell body located in deep lamina II or lamina III. Dendritic distribution is dorsal and terminate in lamina I (Maxwell et al., 2007). (7) Unclassified cell: Unclassified cells are those that do not fit the categories above.

Results

Genetically precise targeting of ChR2 to nonpeptidergic *Mrgprd*$^+$ nociceptive neurons

Mrgprd is expressed in nonpeptidergic polymodal nociceptive neurons that innervate the skin and lamina II of the dorsal spinal cord (Dong et al., 2001; Zylka et al., 2003, 2005; Rau et al., 2009). To selectively express ChR2 in this subset of nociceptive neurons, we targeted the H134R mutant of ChR2-Venus to the *Mrgprd* locus using homologous recombination in embryonic stem cells and then generated *Mrgprd*$\Delta^{hChR2(H134R)Venus}$ (henceforth abbreviated *Mrgprd-ChR2-Venus*) knock-in mice. We found that the ChR2 H134R mutant conducts 3.0-fold more peak and 4.1-fold more steady-state current in HEK293 cells when compared with wild-type ChR2 (data not shown), consistent with previous studies (Nagel et al., 2005; Gradinaru et al., 2007).

To determine whether *Mrgprd-ChR2-Venus* was expressed in nonpeptidergic neurons, we triple stained DRG and spinal cord sections from *Mrgprd-ChR2-Venus* mice with antibodies to GFP (which also detect Venus), the plant lectin IB4 and antibodies to CGRP. Consistent with our previous studies (Zylka et al., 2005), virtually all (99.6%) *Mrgprd-ChR2-Venus*$^+$ neurons were labeled with the nonpeptidergic neuron marker IB4 (Fig. 1*A–D*, arrowheads) whereas few (3.8%) contained high levels of the peptidergic neuron marker CGRP. Conversely, *Mrgprd-ChR2-Venus* was expressed in 81.5% of all IB4$^+$ neurons and 4.0% of all strongly CGRP$^+$ neurons (>290 cells counted per marker combination).

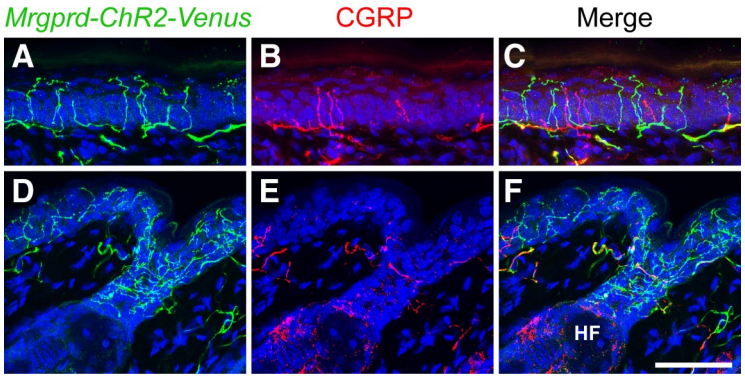

Figure 2. Localization of *Mrgprd-ChR2-Venus* to nerve terminals in glabrous and hairy skin. ***A–F***, Mouse glabrous skin (***A–C***) and hairy skin (***D–F***) were stained with antibodies against GFP (green) and CGRP (red). Nuclei were stained with Draq5 (blue). Images were acquired by confocal microscopy. In ***D–F***, *Mrgprd-ChR2-Venus*$^+$ endings are located in the epidermis and at the neck of a hair follicle (HF). Scale bar, 50 μm.

In addition, ChR2-Venus was colocalized with the nonpeptidergic marker IB4 on axon terminals in lamina II of the spinal cord (Fig. 1*E*,*F*,*H*). There was little overlap between ChR2-Venus and peptidergic CGRP$^+$ terminals in dorsal spinal cord (Fig. 1*E*,*G*,*H*). ChR2-Venus was also localized to free nerve endings in glabrous and hairy skin (Fig. 2). In the glabrous skin, these endings were morphologically distinct from CGRP$^+$ endings and terminated in the outermost living cell layer of epidermis, the stratum granulosum (Fig. 2*A–C*). Collectively, these histochemical studies indicated that ChR2-Venus was selectively expressed in nonpeptidergic *Mrgprd*$^+$ neurons and labeled peripheral and central axon terminals as effectively as membrane-targeted axonal tracers (Leighton et al., 2001; Zylka et al., 2005).

Photostimulation of *Mrgprd*$^+$ DRG neurons in culture

Since ChR2-Venus was expressed in *Mrgprd*$^+$ DRG neurons, this suggested it might be possible to photostimulate *Mrgprd*$^+$ neurons. To test this, we performed whole-cell recordings with dissociated DRG neurons from our *Mrgprd-ChR2-Venus* mice (Fig. 3*A*, inset). All *Mrgprd-ChR2-Venus*$^+$ neurons (identified using intrinsic Venus fluorescence) from heterozygous and homozy-

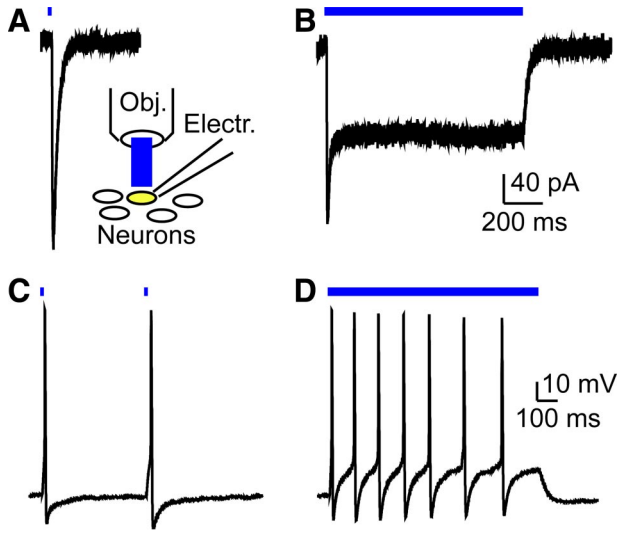

Figure 3. Generation of light-evoked currents and action potentials in *Mrgprd-ChR2-Venus*$^+$ DRG neurons. ***A***, Inset, Recording configuration for all panels. ***A***, ***B***, Voltage-clamp recordings from heterozygous *Mrgprd-ChR2-Venus*$^+$ DRG neuron held at −60 mV and stimulated with blue light for 4 ms (***A***) or 1 s (***B***). ***C***, ***D***, Current-clamp recordings from a heterozygous *Mrgprd-ChR2-Venus*$^+$ neuron stimulated with blue light at 2 Hz for a 4 ms pulse duration (***C***) or for 1 s (***D***). Electr., Electrode; Obj., objective.

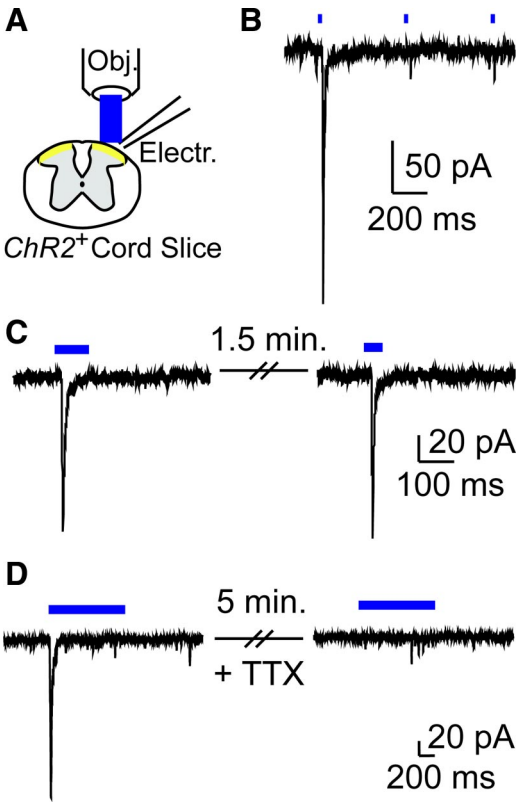

Figure 4. Generation of light-evoked EPSCs in SG neurons and dependence on sodium channel activity. ***A***, Transverse spinal cord slice recording configuration for all panels. Electr., Electrode; Obj., objective. ***B***, Voltage-clamp recording from an SG neuron in an *Mrgprd-ChR2-Venus*$^{-/-}$ spinal cord slice, stimulated with 2 Hz pulsed light. ***C***, Successive $EPSC_L$s from an SG neuron in an *Mrgprd-ChR2-Venus*$^{-/-}$ mouse spinal cord slice. Delay between light presentations was 1.5 min. ***D***, $EPSC_L$ in an SG neuron from an *Mrgprd-ChR2-Venus*$^{-/-}$ mouse was blocked by 5 min bath application of 0.5 μM TTX.

gous mice ($n = 18$ and 11 neurons, respectively) displayed light-evoked photocurrents upon brief (4 ms) and prolonged (1 s) illumination (Fig. 3*A*,*B*). Heterozygous mice express one copy of ChR2 whereas homozygous mice express two copies of ChR2. In addition, light stimulation evoked action potentials in 68% (17 of 25 neurons) and 94% (29 of 31 neurons) of all *Mrgprd-ChR2-Venus*$^+$ DRG neurons from heterozygotes and homozygotes, respectively. In heterozygotes, the maximum firing rate was 2 Hz for pulsed light (Fig. 3*C*) and 7 Hz for continuous illumination (Fig. 3*D*). In homozygotes, the maximum firing rate was 7 Hz for pulsed light and 13 Hz for continuous illumination (data not shown). The latency between light-onset and action potential peak in *Mrgprd-ChR2-Venus*$^{+/-}$ and *Mrgprd-ChR2-Venus*$^{-/-}$ DRG neurons was 21.0 ± 1.4 ms ($n = 17$ spikes) and 19.9 ± 0.3 ms ($n = 190$ spikes), respectively. The spike jitter (average SD of the light-evoked spike latency from each neuron) of *Mrgprd-ChR2-Venus*$^{-/-}$ DRG neurons ($n = 20$) was 1.3 ± 0.3 ms. We did not observe photocurrents or light-evoked action potentials in neurons lacking ChR2.

Mrgprd$^+$ neurons are monosynaptically coupled to most known classes of SG neurons

Considering that *Mrgprd-ChR2-Venus*$^+$ neurons can be "optogenetically" activated, this suggested it might be possible to identify the postsynaptic targets of *Mrgprd*$^+$ neurons using ChR2-assisted circuit mapping (Petreanu et al., 2007). This technique can be used to map connections between presynaptic ChR2$^+$ axons (even when they are severed from their cell bodies in tissue slices) and their postsynaptic targets. Moreover, this technique can be used to assess whether connectivity is monosynaptic or polysynaptic based on spike jitter. First, we assessed whether light-evoked EPSCs ($EPSC_L$s) could be generated in spinal cord slices from *Mrgprd-ChR2-Venus* mice (Fig. 4*A*). We exclusively recorded from neurons in lamina II (the substantia gelatinosa or SG) of spinal cord because anatomical studies suggest *Mrgprd*$^+$ afferents terminate in lamina II but not deeper lamina (Fig. 1*E*) (Zylka et al., 2005). We found that brief light pulses evoked a single $EPSC_L$ in 50% (4 of 8 neurons) and 50% (134 of 269 neurons) of the SG neurons from heterozygous and homozygous mice, respectively (Figs. 4, 5). Excitatory connectivity is consistent with previous studies showing that all DRG neurons are glutamatergic and evoke AMPA receptor-dependent EPSCs when stimulated (Jahr and Jessell, 1985; Schneider and Perl, 1985; Yoshimura and Jessell, 1990). These $EPSC_L$s were exclusively generated as a result of photostimulation of *Mrgprd-ChR2-Venus*$^+$ axon terminals because DRG neurons were not attached to the slices. No $EPSC_L$s were generated in slices from wild-type mice. Low-frequency light pulses failed to generate multiple large amplitude $EPSC_L$s (Fig. 4*B*). However, additional single $EPSC_L$s could be generated by introducing a 0.5–1.5 min delay between light presentations (Fig. 4*C*). And, in most neurons, these $EPSC_L$s were similar in amplitude following each light pulse (Figs. 4*C*, 5). Bath application of the sodium channel blocker tetrodotoxin (TTX; 0.5 μM) inhibited $EPSC_L$s in all SG neurons tested ($n = 3$) (Fig. 4*D*), indicating that $EPSC_L$s were caused by sodium-dependent action potentials in *Mrgprd*$^+$ axon terminals. These TTX experiments ruled out the possibility that $EPSC_L$s were caused by calcium influx through ChR2 (Nagel et al., 2003) followed by direct stimulation of calcium-dependent neurotransmitter release. TTX does not block ChR2 photocurrents (Zhang and Oertner, 2007; Kuhlman and Huang, 2008) but did block $EPSC_L$s, thus ruling out the possibility that $EPSC_L$s were due to ectopic expression of ChR2 in SG neurons. Last, ChR2-Venus was not present in the somas of SG neurons (Fig. 1*E*), further ruling out ectopic expression of ChR2-Venus.

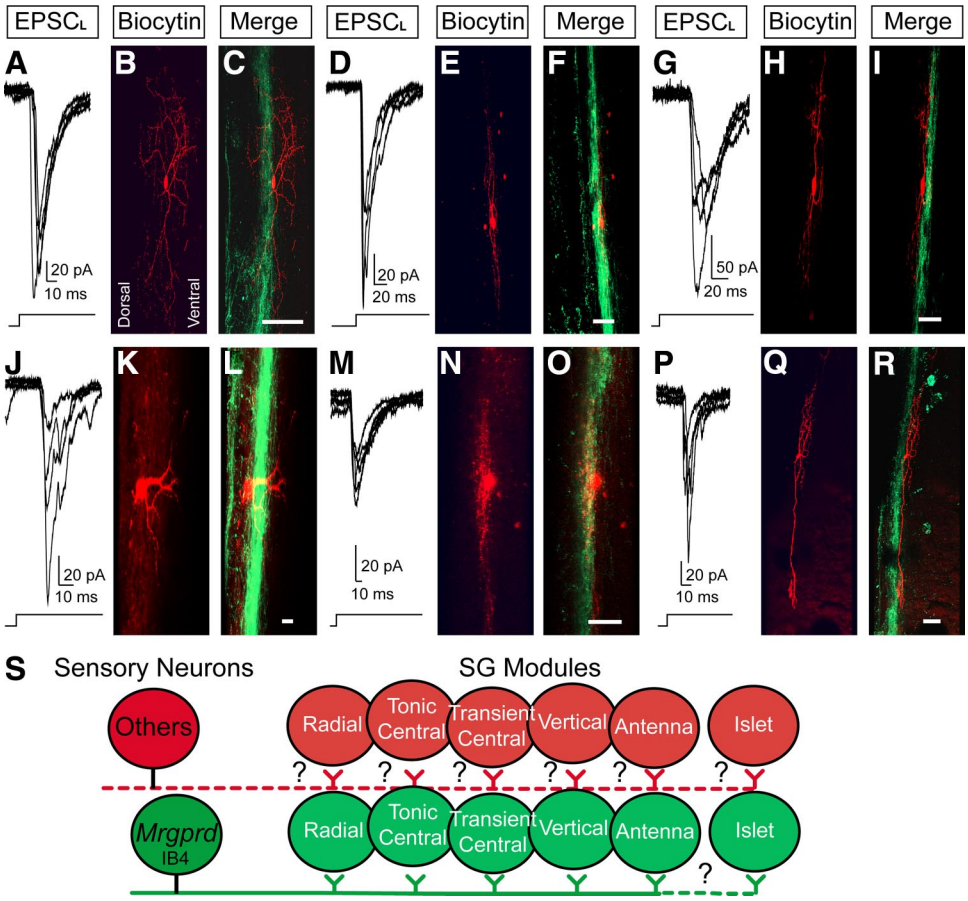

Figure 5. Light-evoked EPSCs can be generated in all known classes of SG neurons. ***A***, ***D***, ***G***, ***J***, ***M***, ***P***, Overlay of five successive $EPSC_L$s from SG neurons in sagittal slices from *Mrgprd-ChR2-Venus*$^{-/-}$ mice. Delay between light presentations was 1 min. Following recording, slices were stained for biocytin (red) and Venus (green, to label *Mrgprd-ChR2-Venus*$^+$ axon terminals) and then imaged by confocal microscopy. Proximity of the recorded neurons to *Mrgprd-ChR2-Venus*$^+$ axon terminals is shown in the merged images. Based on physiological and morphological criteria, neurons were classified as radial (***A–C***), tonic central (***D–F***), transient central (***G–I***), vertical (***J–L***), antenna (***M–O***), and islet (***P–R***). Dorsal is to the left and rostral is toward top for all panels. Scale bar, 50 μm. ***S***, Our data suggest that *Mrgprd*$^+$ afferents innervate "SG modules" made up of most known SG cell types, with the possible exception of islet cells. Since not all SG neurons are monosynaptically connected to *Mrgprd*$^+$ neurons, additional SG modules may exist for other sensory neuron subtypes. Whether these additional SG modules are made up of all known SG cell types or subsets is unknown (indicated by question marks).

Next, to determine whether *Mrgprd*$^+$ neurons were monosynaptically connected to some or all known classes of SG neurons, we repeatedly stimulated SG neurons in slices from homozygous mice with light (five 1000 ms pulses, 1 min interpulse interval) to quantify $EPSC_L$ latency and spike jitter. We also characterized light-responsive SG cells using morphological and physiological criteria (see Materials and Methods). Unlike spike latency, spike jitter provides a reliable means to discriminate monosynaptic from polysynaptic connections (Li and Perl, 1994; Doyle and Andresen, 2001). We classified a connection as monosynaptic in slices from homozygous mice if (1) the $EPSC_L$ spike jitter from a given SG neuron was equal to or less than the upper limit of the light-evoked spike jitter (1.6 ms) from homozygous *Mrgprd-ChR2-Venus*$^+$ DRG neurons and (2) *Mrgprd-ChR2-Venus*$^+$ axon terminals were in close proximity to the soma or dendrites of the recorded SG neuron. Based on these restrictive criteria, we found that *Mrgprd*$^+$ neurons were monosynaptically coupled to most of the known SG cell classes, including radial, tonic central, transient central, vertical, and antenna cells (Table 1, Fig. 5*A–R*). The only known SG cell class that was not monosynaptically coupled to *Mrgprd*$^+$ neurons was the islet cell class (Table 1). In most cases, SG neurons that received monosynaptic input from *Mrgprd*$^+$ neurons also received their primary input from unmyelinated fibers (C-fibers), as assessed by dorsal root stimulation and conduction velocity (Table 1). This is consistent with the termination pattern of unmyelinated afferents in the SG and with the observation that all *Mrgprd*$^+$ afferents are unmyelinated when imaged by electron microscopy (Sugiura et al., 1986; Zylka et al., 2005). In addition, we found that the somas and/or dendritic fields of all light-responsive SG neurons were in close proximity to *Mrgprd*-ChR2-Venus$^+$ axon terminals (Fig. 5*A–R*), further supporting a postsynaptic arrangement relative to *Mrgprd*$^+$ afferents.

Discussion

Mrgprd marks a population of cutaneous polymodal nociceptive neurons that are required for the full expression of mechanical nociception (Zylka et al., 2005; Dussor et al., 2008; Cavanaugh et al., 2009; Rau et al., 2009). In addition, *Mrgprd*$^+$ afferents exclusively terminate in lamina II of the spinal cord, in close proximity to SG neurons (Zylka et al., 2005). This anatomical finding suggested, but did not prove, that nonpeptidergic *Mrgprd*$^+$ neurons innervate SG neurons. Subsequently, using a genetically encoded transneuronal tracer, Braz and colleagues found that nonpeptidergic nociceptive neurons (many of which are likely to be *Mrgprd*$^+$) synapse with a subset of SG neurons in the mouse (Braz et al., 2005). Considering that there are several morphologically and physiologically distinct classes of SG neurons (Grudt

Table 1. Physiological properties of SG neurons that displayed light-evoked EPSCs from *Mrgprd-ChR2-Venus*$^{-/-}$ mice

Cell	Classification	AP pattern	$EPSC_L$ latency ± jitter ± SEM (ms)	Fiber input
1	**Radial**	**Tonic**	**17.7 ± 0.9 ± 0.4**	**C**
2	**Radial**	**Tonic**	**22.8 ± 0.9 ± 0.5**	**Aδ**
3	**Radial**	**Tonic**	**10.4 ± 0.2 ± 0.1**	**C**
4	**Radial**	**Tonic**	**10.8 ± 0.5 ± 0.2**	**C**
5	**Radial**	**Tonic**	**16.5 ± 1.6 ± 0.7**	**C**
6	**Radial**	**Tonic**	**12.8 ± 1.6 ± 0.7**	**C**
7	**Radial**	**Tonic**	**13.2 ± 0.3 ± 0.2**	**C**
8	Radial	Tonic	66.6 ± 32.5 ± 16.2*	C
9	**Tonic central**	**Tonic**	**20.4 ± 0.7 ± 0.3**	**C**
10	**Tonic central**	**Tonic**	**10.4 ± 0.2 ± 0.1**	**C**
11	**Tonic central**	**Tonic**	**23.1 ± 1.2 ± 0.5**	**Ambiguous**
12	**Tonic central**	**Tonic**	**21.9 ± 1.2 ± 0.5**	**C**
13	**Tonic central**	**Tonic**	**20.2 ± 1.5 ± 0.7**	**C**
14	**Tonic central**	**Tonic**	**20.1 ± 1.5 ± 0.7**	**C**
15	**Tonic central**	**Tonic**	**16.9 ± 0.8 ± 0.4**	**C**
16	**Tonic central**	**Tonic**	**18.4 ± 0.9 ± 0.4**	**C**
17	Tonic central	Tonic	23.7 ± 3.3 ± 1.5*	C
18	Tonic central	Tonic	24.5 ± 2.6 ± 1.1*	C
19	Tonic central	Tonic	57.7 ± 19.3 ± 8.6*	C
20	Tonic central	Tonic	18.5 ± 2.1 ± 1.5*	C
21	Tonic central	Tonic	39.8 ± 5.8 ± 2.6*	C
22	**Transient central**	**Transient**	**15.0 ± 1.0 ± 0.4**	**C**
23	**Transient central**	**Transient**	**20.3 ± 1.0 ± 0.5**	**C**
24	Transient central	Transient	14.5 ± 2.5 ± 1.1*	C
25	Transient central	Transient	21.6 ± 2.2 ± 1.0*	C
26	Transient central	Transient	25.7 ± 4.2 ± 1.9*	C
27	Transient central	Transient	47.1 ± 4.1 ± 1.8*	C
28	Transient central	Transient	22.3 ± 2.0 ± 0.9*	C
29	**Vertical**	**Delayed**	**18.8 ± 1.4 ± 0.6**	**C**
30	Vertical	Tonic	26.6 ± 2.3 ± 1.2*	C
31	Vertical	Delayed	29.7 ± 2.4 ± 1.1*	Ambiguous
32	Vertical	Delayed	23.6 ± 4.0 ± 3.4*	Ambiguous
33	Vertical	Delayed	18.5 ± 2.0 ± 0.9*	C
34	Vertical	Delayed	23.4 ± 2.4 ± 1.1*	C
35	**Antenna**	**Tonic**	**12.9 ± 1.4 ± 0.6**	**C**
36	Islet	Tonic	19.8 ± 2.5 ± 1.1*	C
37	**Unclassified**	**Tonic**	**11.5 ± 0.4 ± 0.2**	**Ambiguous**
38	Unclassified	Tonic	24.5 ± 2.0 ± 1.0*	C
39	Unclassified	Transient	17.7 ± 2.1 ± 1.0*	C
40	Unclassified	Transient	34.6 ± 2.9 ± 1.4*	C

Boldface, monosynaptic; marked with asterisk, polysynaptic. Ambiguous: dorsal root too short to accurately calculate conduction velocity.

and Perl, 2002; Maxwell et al., 2007), this raises the question of whether nonpeptidergic neurons innervate a homogeneous or heterogeneous subset of SG neurons. Currently, there are no molecular markers that uniquely distinguish each known SG cell type. In an effort to identify the postsynaptic targets of *Mrgprd*$^+$ neurons, we genetically targeted the light-activated ion channel ChR2-Venus to *Mrgprd*$^+$ DRG neurons. This allowed us to precisely control the electrical activity of this subset of nociceptive neurons and map connectivity using morphological and physiological criteria. Unlike the standard approach of classifying afferent input as myelinated (Aβ, Aδ) or unmyelinated (C-fiber) by stimulating the dorsal root with suction electrodes, our use of ChR2 allowed us to selectively stimulate a genetically defined class of unmyelinated afferent.

First, we found that ChR2-Venus was expressed in nonpeptidergic *Mrgprd*$^+$ DRG neurons and labeled the central and peripheral terminals of these neurons as effectively as genetically encoded axonal tracers (Zylka et al., 2005). In addition, we found that light-evoked action potentials could be generated in a majority of all *Mrgprd-ChR2-Venus*$^+$ DRG neurons regardless of whether one or two copies of ChR2 were expressed.

Using whole-cell recordings from spinal cord slices, we found that light-evoked EPSCs could be generated in 50% (134 of 269) of all SG neurons from *Mrgprd-ChR2-Venus* homozygous mice. Our inability to generate $EPSC_L$s in the remaining SG neurons was not due to recording of cells outside the SG because the borders of the SG are clearly visible under IR-DIC illumination. In addition, our inability to generate $EPSC_L$s in the remaining SG neurons was not due to inefficient activation of ChR2$^+$ axon terminals. A similar percentage of SG neurons were activated in heterozygous and homozygous mice [although the number of SG neurons recorded from heterozygotes ($n = 8$; vs $n = 269$ from homozygotes) was too low to permit a statistical comparison]. If activation was inefficient, $EPSC_L$s should have been generated in a smaller percentage of SG neurons from heterozygotes compared with homozygotes since the percentage of ChR2$^+$ DRG neurons that displayed light-evoked action potentials scaled with ChR2 expression level (68% of all ChR2-Venus$^+$ neurons in heterozygotes, 94% of all ChR2-Venus$^+$ neurons in homozygotes). Moreover, poor cell health could not account for this lack of activation because all of the recorded neurons were healthy by electrophysiological criteria (current-clamp: stable input resistance, resting membrane potential was −40 mV or lower, and neurons fired action potentials with overshoot upon current injection; voltage-clamp: holding current was <50 pA, series resistance was <30 MΩ). Instead, these nonresponsive neurons, which account for 50% of all SG neurons, might be innervated by other molecularly, anatomically, and functionally unique classes of sensory neurons, such as peptidergic afferents, IB4$^+$ afferents that do not express *Mrgprd* (represents ~25% of the nonpeptidergic IB4$^+$ population), TRPV1$^+$ afferents, visceral afferents, and/or *Mrgprb4*$^+$ afferents (Fig. 5*S*) (Caterina et al., 1997; Molliver et al., 1997; Zylka et al., 2005; Liu et al., 2007).

Surprisingly, our studies revealed that *Mrgprd*$^+$ neurons were monosynaptically connected with almost all known SG cell types, with the possible exception of islet cells (Fig. 5*S*). This makes it unlikely that molecularly distinct primary sensory neurons synapse exclusively with a homogeneous, dedicated class of SG neuron. Instead, our data suggest molecularly and functionally distinct classes of primary sensory neurons may interface with "SG modules" made up of multiple SG neuron classes (Fig. 5*S*). This modular organization for afferent input is supported by our observation that only half all SG neurons are light-responsive and, of these light-responsive SG neurons, only ~50% (Table 1) are monosynaptically coupled to *Mrgprd*$^+$ neurons. This suggests that not all SG neurons receive direct *Mrgprd*$^+$ afferent input. These nonresponsive SG neurons might receive input from other classes of sensory neurons. SG neurons are themselves organized as stereotyped, modular circuits made up of identifiable presynaptic and postsynaptic neurons (Lu and Perl, 2003, 2005). Thus, an "SG module" may represent a minimal circuit element that is dedicated to processing modality-selective information in the dorsal horn.

This modular organization could not have been identified using anatomy or molecular markers alone, especially given that no molecular markers exist for every SG neuron class. At present, only a subset of tonic central cells can be genetically marked using prion promoter-GFP transgenic mice (Hantman et al., 2004). And, a relatively inhomogeneous SG neuron population is labeled in GAD67-GFP transgenic mice (Heinke et al., 2004).

A modular organization for afferent input has obvious functional and behavioral implications. For example, *Mrgprb4* and *Mrgprd* are both members of the Mas-related GPCR family and are expressed in distinct populations of DRG neurons (Dong et

al., 2001; Zylka et al., 2003). These molecularly distinct neurons innervate different regions of the skin, have terminals that intermingle in lamina II, and likely encode unique stimulus modalities (Zylka et al., 2005; Liu et al., 2007). *Mrgprd*$^+$ neurons are unmyelinated polymodal nociceptors and are required for full behavioral responsiveness to noxious mechanical stimuli (Cavanaugh et al., 2009; Rau et al., 2009). In contrast, *Mrgprb4*$^+$ neurons are unmyelinated and are hypothesized to be low-threshold mechanoreceptors that encode pleasurable touch (Bessou and Perl, 1969; Light et al., 1979; Olausson et al., 2002; Liu et al., 2007; Löken et al., 2009). Thus, SG circuit modules could serve to segregate somatosensory information that is sensed and perceived as distinct.

We encountered only one islet cell that was driven by photostimulation, although it was not monosynaptically coupled to *Mrgprd*$^+$ neurons by our restrictive criteria (Table 1). Given that islet cells are relatively common in the SG, representing ~16% of all SG neurons (Todd and Lewis, 1986; Grudt and Perl, 2002; Yasaka et al., 2007), this suggests that *Mrgprd*$^+$ afferents are either not connected or only sparsely connected with islet cells. Interestingly, Perl and Lu found that islet cells are innervated by a more rapidly conducting population of C-fibers whereas central cells are innervated by a more slowly conducting C-fiber class (Lu and Perl, 2003). Based on the known conduction velocities of sensory afferents, Perl and Lu hypothesized that islet cells were preferentially innervated by low-threshold mechanoreceptors or cooling thermoreceptors whereas central cells were innervated by nociceptors. Our present data support this hypothesis as *Mrgprd*$^+$ neurons function as cutaneous polymodal nociceptors (Rau et al., 2009) and connections between *Mrgprd* afferents and central cells were common (Table 1). It is tempting to speculate that *Mrgprb4*$^+$ neurons, which represent putative unmyelinated low-threshold mechanoreceptors (Liu et al., 2007), might disproportionately innervate islet cells. Islet cells are inhibitory and have a dendritic arbor that is approximately twice as long in the rostral–caudal dimension when compared with other SG cell types (Grudt and Perl, 2002). This could facilitate integration of somatosensory information over a larger area of the body. Perhaps not coincidentally, *Mrgprb4*$^+$ neurons and low-threshold mechanoreceptors have receptive fields that are larger than the receptive fields of nociceptive neurons (Bessou and Perl, 1969; Wessberg et al., 2003; Liu et al., 2007).

Ultimately, additional studies will be needed to determine whether other molecularly and physiologically distinct subsets of sensory neurons interface with dedicated SG modules and whether there is cross talk between these modules. This could be addressed by targeting spectrally distinct ChR2 variants to other molecularly defined subsets of sensory neurons (Zhang et al., 2008). Considering that there are excitatory and inhibitory connections between SG cell types (Lu and Perl, 2003, 2005; Yasaka et al., 2007; Kato et al., 2009), SG modules may not only segregate distinct stimulus modalities in the CNS but also facilitate activation and inhibition across stimulus modalities. This circuit organization supports labeled line and convergent mechanisms for processing pain signals and could underlie sensory phenomena that incorporate cross-modality interactions, including itch-mediated inhibition of pain and the thermal grill illusion (Craig, 2002, 2003).

References

Arenkiel BR, Peca J, Davison IG, Feliciano C, Deisseroth K, Augustine GJ, Ehlers MD, Feng G (2007) In vivo light-induced activation of neural circuitry in transgenic mice expressing channelrhodopsin-2. Neuron 54:205–218.

Bessou P, Perl ER (1969) Response of cutaneous sensory units with unmyelinated fibers to noxious stimuli. J Neurophysiol 32:1025–1043.

Bi A, Cui J, Ma YP, Olshevskaya E, Pu M, Dizhoor AM, Pan ZH (2006) Ectopic expression of a microbial-type rhodopsin restores visual responses in mice with photoreceptor degeneration. Neuron 50:23–33.

Boyden ES, Zhang F, Bamberg E, Nagel G, Deisseroth K (2005) Millisecond-timescale, genetically targeted optical control of neural activity. Nat Neurosci 8:1263–1268.

Braz JM, Nassar MA, Wood JN, Basbaum AI (2005) Parallel "pain" pathways arise from subpopulations of primary afferent nociceptor. Neuron 47:787–793.

Bunting M, Bernstein KE, Greer JM, Capecchi MR, Thomas KR (1999) Targeting genes for self-excision in the germ line. Genes Dev 13:1524–1528.

Campagnola L, Wang H, Zylka MJ (2008) Fiber-coupled light-emitting diode for localized photostimulation of neurons expressing channelrhodopsin-2. J Neurosci Methods 169:27–33.

Caterina MJ, Schumacher MA, Tominaga M, Rosen TA, Levine JD, Julius D (1997) The capsaicin receptor: a heat-activated ion channel in the pain pathway. Nature 389:816–824.

Cavanaugh DJ, Lee H, Lo L, Shields SD, Zylka MJ, Basbaum AI, Anderson DJ (2009) Distinct subsets of unmyelinated primary sensory fibers mediate behavioral responses to noxious thermal and mechanical stimuli. Proc Natl Acad Sci U S A 106:9075–9080.

Craig AD (2002) How do you feel? Interoception: the sense of the physiological condition of the body. Nat Rev Neurosci 3:655–666.

Craig AD (2003) Pain mechanisms: labeled lines versus convergence in central processing. Annu Rev Neurosci 26:1–30.

Dong X, Han S, Zylka MJ, Simon MI, Anderson DJ (2001) A diverse family of GPCRs expressed in specific subsets of nociceptive sensory neurons. Cell 106:619–632.

Doyle MW, Andresen MC (2001) Reliability of monosynaptic sensory transmission in brain stem neurons in vitro. J Neurophysiol 85:2213–2223.

Dussor G, Zylka MJ, Anderson DJ, McCleskey EW (2008) Cutaneous sensory neurons expressing the Mrgprd receptor sense extracellular ATP and are putative nociceptors. J Neurophysiol 99:1581–1589.

Gradinaru V, Thompson KR, Zhang F, Mogri M, Kay K, Schneider MB, Deisseroth K (2007) Targeting and readout strategies for fast optical neural control *in vitro* and *in vivo*. J Neurosci 27:14231–14238.

Grudt TJ, Perl ER (2002) Correlations between neuronal morphology and electrophysiological features in the rodent superficial dorsal horn. J Physiol 540:189–207.

Hantman AW, van den Pol AN, Perl ER (2004) Morphological and physiological features of a set of spinal substantia gelatinosa neurons defined by green fluorescent protein expression. J Neurosci 24:836–842.

Heinke B, Ruscheweyh R, Forsthuber L, Wunderbaldinger G, Sandkühler J (2004) Physiological, neurochemical and morphological properties of a subgroup of GABAergic spinal lamina II neurones identified by expression of green fluorescent protein in mice. J Physiol 560:249–266.

Hunt SP, Mantyh PW (2001) The molecular dynamics of pain control. Nat Rev Neurosci 2:83–91.

Hwang RY, Zhong L, Xu Y, Johnson T, Zhang F, Deisseroth K, Tracey WD (2007) Nociceptive neurons protect *Drosophila* larvae from parasitoid wasps. Curr Biol 17:2105–2116.

Jahr CE, Jessell TM (1985) Synaptic transmission between dorsal root ganglion and dorsal horn neurons in culture: antagonism of monosynaptic excitatory postsynaptic potentials and glutamate excitation by kynurenate. J Neurosci 5:2281–2289.

Karai L, Brown DC, Mannes AJ, Connelly ST, Brown J, Gandal M, Wellisch OM, Neubert JK, Olah Z, Iadarola MJ (2004) Deletion of vanilloid receptor 1-expressing primary afferent neurons for pain control. J Clin Invest 113:1344–1352.

Kato G, Kawasaki Y, Koga K, Uta D, Kosugi M, Yasaka T, Yoshimura M, Ji RR, Strassman AM (2009) Organization of intralaminar and translaminar neuronal connectivity in the superficial spinal dorsal horn. J Neurosci 29:5088–5099.

Kuhlman SJ, Huang ZJ (2008) High-resolution labeling and functional manipulation of specific neuron types in mouse brain by Cre-activated viral gene expression. PLoS One 3:e2005.

Leighton PA, Mitchell KJ, Goodrich LV, Lu X, Pinson K, Scherz P, Skarnes WC, Tessier-Lavigne M (2001) Defining brain wiring patterns and mechanisms through gene trapping in mice. Nature 410:174–179.

Li J, Perl ER (1994) Adenosine inhibition of synaptic transmission in the substantia gelatinosa. J Neurophysiol 72:1611–1621.

Li X, Gutierrez DV, Hanson MG, Han J, Mark MD, Chiel H, Hegemann P, Landmesser LT, Herlitze S (2005) Fast noninvasive activation and inhibition of neural and network activity by vertebrate rhodopsin and green algae channelrhodopsin. Proc Natl Acad Sci U S A 102:17816–17821.

Liewald JF, Brauner M, Stephens GJ, Bouhours M, Schultheis C, Zhen M, Gottschalk A (2008) Optogenetic analysis of synaptic function. Nat Methods 5:895–902.

Light AR, Trevino DL, Perl ER (1979) Morphological features of functionally defined neurons in the marginal zone and substantia gelatinosa of the spinal dorsal horn. J Comp Neurol 186:151–171.

Liu Q, Vrontou S, Rice FL, Zylka MJ, Dong X, Anderson DJ (2007) Molecular genetic visualization of a rare subset of unmyelinated sensory neurons that may detect gentle touch. Nat Neurosci 10:946–948.

Löken LS, Wessberg J, Morrison I, McGlone F, Olausson H (2009) Coding of pleasant touch by unmyelinated afferents in humans. Nat Neurosci 12:547–548.

Lu Y, Perl ER (2003) A specific inhibitory pathway between substantia gelatinosa neurons receiving direct C-fiber input. J Neurosci 23:8752–8758.

Lu Y, Perl ER (2005) Modular organization of excitatory circuits between neurons of the spinal superficial dorsal horn (laminae I and II). J Neurosci 25:3900–3907.

Maxwell DJ, Belle MD, Cheunsuang O, Stewart A, Morris R (2007) Morphology of inhibitory and excitatory interneurons in superficial laminae of the rat dorsal horn. J Physiol 584:521–533.

Molliver DC, Wright DE, Leitner ML, Parsadanian AS, Doster K, Wen D, Yan Q, Snider WD (1997) IB4-binding DRG neurons switch from NGF to GDNF dependence in early postnatal life. Neuron 19:849–861.

Nagel G, Szellas T, Huhn W, Kateriya S, Adeishvili N, Berthold P, Ollig D, Hegemann P, Bamberg E (2003) Channelrhodopsin-2, a directly light-gated cation-selective membrane channel. Proc Natl Acad Sci U S A 100:13940–13945.

Nagel G, Brauner M, Liewald JF, Adeishvili N, Bamberg E, Gottschalk A (2005) Light activation of channelrhodopsin-2 in excitable cells of *Caenorhabditis elegans* triggers rapid behavioral responses. Curr Biol 15:2279–2284.

Olausson H, Lamarre Y, Backlund H, Morin C, Wallin BG, Starck G, Ekholm S, Strigo I, Worsley K, Vallbo AB, Bushnell MC (2002) Unmyelinated tactile afferents signal touch and project to insular cortex. Nat Neurosci 5:900–904.

Perl ER (1996) Cutaneous polymodal receptors: characteristics and plasticity. In: Progress in brain research (Kumazawa T, Kruger L, Mizumura K, eds), pp 21–37. Amsterdam: Elsevier.

Petreanu L, Huber D, Sobczyk A, Svoboda K (2007) Channelrhodopsin-2-assisted circuit mapping of long-range callosal projections. Nat Neurosci 10:663–668.

Rau KK, McIlwrath SL, Wang H, Lawson JJ, Jankowski MP, Zylka MJ, Anderson DJ, Koerber HR (2009) Mrgprd enhances excitability in specific populations of cutaneous murine polymodal nociceptors. J Neurosci 29:8612–8619.

Schneider SP, Perl ER (1985) Selective excitation of neurons in the mammalian spinal dorsal horn by aspartate and glutamate in vitro: correlation with location and excitatory input. Brain Res 360:339–343.

Sugiura Y, Lee CL, Perl ER (1986) Central projections of identified, unmyelinated (C) afferent fibers innervating mammalian skin. Science 234:358–361.

Todd AJ, Lewis SG (1986) The morphology of Golgi-stained neurons in lamina II of the rat spinal cord. J Anat 149:113–119.

Wang H, Peca J, Matsuzaki M, Matsuzaki K, Noguchi J, Qiu L, Wang D, Zhang F, Boyden E, Deisseroth K, Kasai H, Hall WC, Feng G, Augustine GJ (2007) High-speed mapping of synaptic connectivity using photostimulation in Channelrhodopsin-2 transgenic mice. Proc Natl Acad Sci U S A 104:8143–8148.

Wessberg J, Olausson H, Fernström KW, Vallbo AB (2003) Receptive field properties of unmyelinated tactile afferents in the human skin. J Neurophysiol 89:1567–1575.

Woolf CJ, Ma Q (2007) Nociceptors–noxious stimulus detectors. Neuron 55:353–364.

Yasaka T, Kato G, Furue H, Rashid MH, Sonohata M, Tamae A, Murata Y, Masuko S, Yoshimura M (2007) Cell-type-specific excitatory and inhibitory circuits involving primary afferents in the substantia gelatinosa of the rat spinal dorsal horn in vitro. J Physiol 581:603–618.

Yoshimura M, Jessell T (1990) Amino acid-mediated EPSPs at primary afferent synapses with substantia gelatinosa neurones in the rat spinal cord. J Physiol 430:315–335.

Zhang F, Prigge M, Beyrière F, Tsunoda SP, Mattis J, Yizhar O, Hegemann P, Deisseroth K (2008) Red-shifted optogenetic excitation: a tool for fast neural control derived from *Volvox carteri*. Nat Neurosci 11:631–633.

Zhang YP, Oertner TG (2007) Optical induction of synaptic plasticity using a light-sensitive channel. Nat Methods 4:139–141.

Zylka MJ, Dong X, Southwell AL, Anderson DJ (2003) Atypical expansion in mice of the sensory neuron-specific Mrg G protein-coupled receptor family. Proc Natl Acad Sci U S A 100:10043–10048.

Zylka MJ, Rice FL, Anderson DJ (2005) Topographically distinct epidermal nociceptive circuits revealed by axonal tracers targeted to Mrgprd. Neuron 45:17–25.

Zylka MJ, Sowa NA, Taylor-Blake B, Twomey MA, Herrala A, Voikar V, Vihko P (2008) Prostatic acid phosphatase is an ectonucleotidase and suppresses pain by generating adenosine. Neuron 60:111–122.